Greater Default-Mode Network Abnormalities Compared to High Order Visual Processing Systems in Amnestic Mild Cognitive Impairment: An Integrated Multi-Modal MRI Study

Roser Sala-Llonch[a,b], Beatriz Bosch[a], Eider M. Arenaza-Urquijo[b], Lorena Rami[a], Núria Bargalló[c,d], Carme Junqué[b,c], José-Luis Molinuevo[a,c] and David Bartrés-Faz[b,c,*]

[a]*Alzheimer's Disease and Other Cognitive Disorders Unit, Neurology Service, Hospital Clínic de Barcelona, Catalonia, Spain*
[b]*Department de Psiquiatria i Psicobiologia Clinica, Universitat de Barcelona, Catalonia, Spain*
[c]*Institut d'Investigacions Biomèdiques August Pi i Sunyer (IDIBAPS), Catalonia, Spain*
[d]*Radiology Service, Hospital Clínic de Barcelona, Catalonia, Spain*

Abstract. We conducted an integrated multi-modal magnetic resonance imaging (MRI) study based on functional MRI (fMRI) data during a complex but cognitively preserved visual task in 15 amnestic mild cognitive impairment (a-MCI) patients and 15 Healthy Elders (HE). Independent Component Analysis of fMRI data identified a functional network containing an Activation Task Related Pattern (ATRP), including regions of the dorsal and ventral visual stream, and a Deactivation Task Related Pattern network (DTRP), with high spatial correspondence with the default-mode network (DMN). Gray matter (GM) volumes of the underlying ATRP and DTRP cortical areas were measured, and probabilistic tractography (based on diffusion MRI) identified fiber pathways within each functional network. For the ATRP network, a-MCI patients exhibited increased fMRI responses in inferior-ventral visual areas, possibly reflecting compensatory activations for more compromised dorsal regions. However, no significant GM or white matter group differences were observed within the ATRP network. For the DTRP/DMN, a-MCI showed deactivation deficits and reduced GM volumes in the posterior cingulate/precuneus, excessive deactivations in the inferior parietal lobe, and less fiber tract integrity in the cingulate bundles. Task performance correlated with DTRP-functionality in the HE group. Besides allowing the identification of functional reorganizations in the cortical network directly processing the task-stimuli, these findings highlight the importance of conducting integrated multi-modal MRI studies in MCI based on spared cognitive domains in order to identify functional abnormalities in critical areas of the DMN and their precise anatomical substrates. These latter findings may reflect early neuroimaging biomarkers in dementia.

Keywords: Alzheimer's disease, compensation, default-mode network, diffusion MRI, fMRI, mild cognitive impairment, structural magnetic resonance, tractography, visual pathways

INTRODUCTION

Mild cognitive impairment (MCI) defines a transitional state between normal aging and dementia and is considered a prodromal stage of Alzheimer's disease (AD) [1], especially when it presents in its amnestic

---

*Correspondence to: David Bartrés-Faz, PhD, Departament de Psiquiatria i Psicobiologia Clinica, Facultat de Medicina, Universitat de Barcelona, Casanova 143, 08036 Barcelona, Spain. Tel.: +34 93 4037264; Fax: +34 93 4035294; E-mail: dbartres@ub.edu.

subtype [2,3]. MCI thus represents an ideal model for broadening our understanding of the early pathophysiology of incipient AD. In recent years, both structural and functional neuroimaging techniques have been extensively applied in order to characterize MCI cross-sectionally, and have identified a set of imaging biomarkers that have predictive value as regards future conversion or clinical stability in these patients [4,5].

Among neuroimaging techniques, functional magnetic resonance imaging (fMRI) is particularly well suited to investigate whether early functional brain reorganizations can be detected prior to overt neuropsychological or structural brain abnormalities [6], and thus reveal subtle cerebral functional adaptations in preclinical dementia. In the MCI context, however, most fMRI studies have considered learning and/or memory paradigms, a cognitive area which by definition is affected in most MCI patients [7–13]. As regards other cognitive domains, a few independent fMRI reports have revealed abnormal patterns of brain activity in attentional and executive domains [14,15] or in language processing [16]. In one recent study [17] the authors integrated the study of language, memory, attention, and empathy in a cohort of a-MCI patients. One promising line of research has centered on the investigation of complex visual processing in MCI patients, given the well-characterized anatomy of the dorsal and ventral visual pathways and the fact that visuospatial and visuoperceptive functions are early affected in AD. These investigations have revealed preclinical functional reorganizations in high order visual areas supporting both visuospatial [18,19] and visuoperceptive [19–22] processing among MCI and early AD. fMRI study of complex visual functions in these patients provides further clinically relevant evidence, as it has been demonstrated that patients who will convert to AD present increased brain responses with increasing task demands in areas related to visuospatial processing, probably reflecting reduced neuronal efficiency due to accumulating AD pathology [18].

In dementia, the optimal use of cerebral networks in terms of cognitive capability strongly depends on the integrity and precise spatio-temporal tuning of their functional and structural components [23]. However, in the study of complex visual functions in MCI, only Teipel and colleagues [21] have investigated system-specific associations between the functional connectivity of neural systems and their underlying morphological features. In their report, those authors observed more positive associations for MCI patients than for controls between gray matter (GM) volumes in regions

of the ventral visual system and fusiform gyrus activity during a face-matching task, as well as negative correlations between this region and anatomical areas outside the ventral visual pathway. That study supported the notion that the functional segregation within the visual system is based on the distribution of cortical GM volumes in MCI patients. However, the investigation restricted the analysis of brain activity to a particular area based on an a priori hypothesis and did not consider structural connectivity as a further measure in the model.

The aim of the present study was to provide the first comprehensive characterization of a functional and structural cerebral network underlying complex visual processing in MCI patients. The primary objective was to determine whether network-related alterations in MCI appear even before clinical impairment in this cognitive domain can be detected. For this purpose, we used three MRI modalities (T1-structural, fMRI, and Diffusion MRI) to perform an integrated analysis including functional connectivity, GM volumetry, and probabilistic tractography. First, the study of task-activated regions allows the characterization of these visual processing related networks. Furthermore, the study of task-deactivations allowed us to investigate the brain's default-mode network (DMN, [24–27]), defined as a set of brain regions showing high levels of functional connectivity with core areas in the anterior/frontal and posterior midline structures as well as in the parietal regions. The DMN is significantly more activated during rest or passive sensory tasks than in cognitively demanding or goal-directed tasks and is known to be compromised in neurodegenerative disorders, including AD, particularly in the posterior cingulate cortex (PCC), an area primarily affected by AD-associated alterations such as hypometabolism or elevated atrophy rate [27]. More recent studies of deactivations in the context of memory tasks [28] or resting state fMRI conditions [29,30] have also noted dysfunction in this system in MCI, but the relationship between functional alterations and their precise underlying structural brain correlates is still largely unknown in this condition.

Briefly, the main steps of the data analyses presented in this paper are as follows. First, we used Independent Component Analysis (ICA) to explore the functional networks involved in the task and functional differences between groups. Importantly, within the main component, regions exhibiting both task-related activations and deactivations were identified, defining two different networks. The spatial maps of the functional networks obtained were then thresholded and several

ROIs defining isolated but functionally connected regions were extracted from them. Furthermore, these ROIs were used to evaluate structural characteristics of the networks such as GM volumes and network-related white matter pathways between pairs of ROI. We investigated differences in these measures as well as relationships between structure and functionality.

METHODS

Subjects

Thirty right-handed subjects aged over 65 were prospectively recruited from the AD and other cognitive disorders unit at the Neurology Service of the Hospital Clinic in Barcelona. The sample comprised 15 healthy elders (HE) and 15 MCI patients. Patients with a clinical diagnosis of AD were not included because the study focused on identifying a brain network related to a preserved cognitive domain, which would have been more difficult to attain with demented patients. MCI patients were prospectively selected only if they presented the amnestic form of the disorder (a-MCI; single memory domain affected), defined by the fact that their remaining cognitive functions and activities of daily living were within the normal range. We used the Pfeffer Functional Activities Questionnaire (FAQ) [31] to assess patients' functional activities. The FAQ comprises 10 items, which evaluate a variety of Activities of Daily Living (ADL) and complex cognitive/social functions. We considered that ADL were impaired if the FAQ score was $\geqslant 3$. All subjects scored < 3 in the FAQ. Healthy individuals did not meet criteria for dementia and presented no cognitive complaints or scores below -1.5 SD on any neuropsychological test. Patients with a-MCI reported complaints of memory function and scores below -1.5 SD on an episodic memory test (long term retrieval test from the FCRST: Free and cued selective reminding test). A comprehensive neuropsychological battery was administered to all subjects, including assessments of memory, frontal lobe 'executive' functions, language, gnosis, and praxis tests [16]. Visuoperceptive-visuospatial functions were assessed by means of the Incomplete Letters and the Number location tests of the Visual Object and Space Perception Battery (VOSP, [32]). Additionally, the Perception Digital Test (PDT) was also administered to evaluate high order visual functions [33]. We verified that all a-MCI patients performed within normal limits in this test, which was adapted for use within the fMRI context (see below).

Finally, all the a-MCI subjects were clinically re-evaluated two years after this first scanning session and it was observed that some of them (5 of 15) had converted to AD.

MRI acquisition

Subjects were examined on a 3T MRI scanner (Magnetom Trio Tim, Siemens Medical Systems, Germany). For the fMRI protocol, 225 T2*-weighted volumes were acquired during the task performance (TR = 2000 ms, TE = 29 ms, 36 slices per volume, slice thickness = 3 mm, distance factor = 25%, FOV = 240 mm, matrix size = 128 × 128). A high resolution 3D structural dataset (T1-weighted MP-RAGE, TR = 2300 ms, TE = 2.98 ms, 240 slices, FOV = 256 mm; matrix size = 256 × 256; Slice thickness = 1 mm) was also acquired, followed by a Diffusion Weighted Imaging (DWI) protocol which consisted of an echo-planar imaging (EPI) sequence (30 directions, TR = 5600 ms, TE = 89 ms, 44 slices, slice thickness = 2 mm, distance factor = 30%, FOV = 250 mm, matrix size = 122 × 122). The DWI protocol also provided a T2-weighted volume (B0) which was used to exclude participants with evidence of cerebrovascular disease based on the evaluation of white matter (WM) hyperintensities. Specifically, a board-certified neuroradiologist (NB) rated all images using the Fazekas scale [34]. Because of this, some WM abnormalities were observed in our sample, probably age-related, as all the participants rated 1–2 on this scale. No differences were observed between the two clinical groups [mean (SD) Fazekas scores were 1.13 (0.74) and 1.06 (0.59) for the HE and a-MCI groups respectively; $t = 0.27, p = 0.78$].

fMRI task

We used a block design paradigm consisting of three alternating conditions. During the experimental condition (10 scans, duration: 20 s) subjects were presented with four blurred images within each of the four quadrants of the screen. Three of the images were rotated 90, −90, and 180 degrees respectively, while the remaining one was randomly positioned in the correct orientation. After correct identification of the content of the images (i.e., visually decoding the picture to identify that it represented, for example, a landscape, an object or people) the subject was asked to answer whether the image that was correctly orientated was on
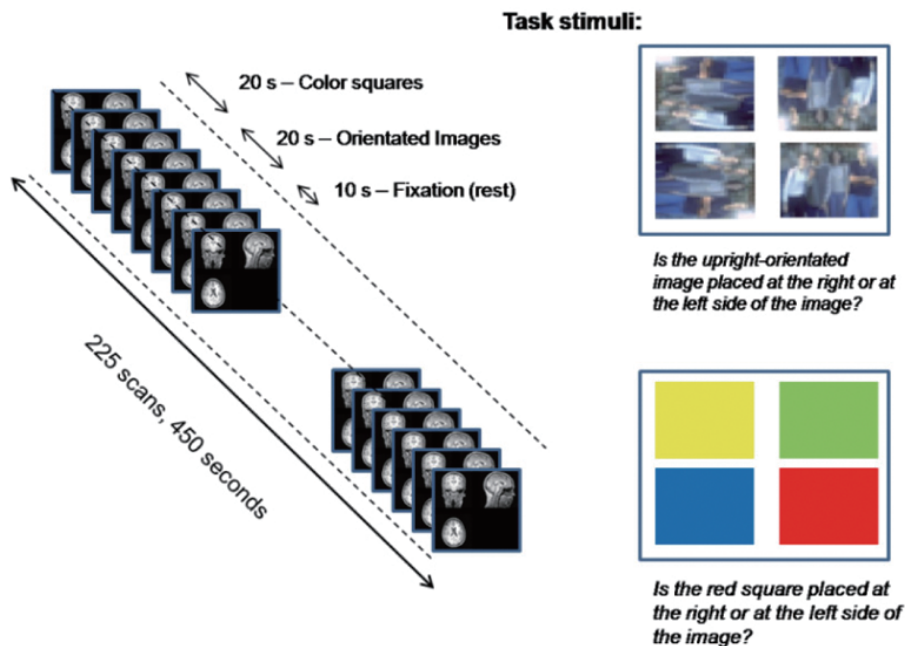
Fig. 1. Design of the fMRI task and stimuli used. Instructions were given to the subjects once, before the scanning session. See main text for full description of the task.

the right or on the left side of the screen by pressing a right/left button. During the control task (10 scans, duration: 20 s), four plain colored squares were presented in the same spatial arrangement as the images of the task stimuli, and the subject was asked to indicate whether the red square was on the right or left side. As instructions were given to the subjects before the scanning session, no written instructions appeared on the screen during the task. The number of right/left responses was equivalent in the experimental and control conditions. Finally, a fixation/resting block was also presented, consisting of a white cross on a black screen (5 scans, duration: 10 s). The whole paradigm included 9 repetitions of the task, with a total duration of 450 s. (Fig. 1).

MRI processing and analyses

All the procedures carried out in the analysis of the three MR modalities used and their inferences are shown in Fig. 2. The functional brain networks extracted from ICA analysis of fMRI data were used to guide GM volumetric and DTI analyses in order to define the anatomical parts of the network. Neuroimaging tools used in all the steps are part of the FSL software (http://www.fmrib.ox.ac.uk/fsl [35]).

Functional MRI processing and analysis

First, each fMRI dataset was corrected for motion using MCFLIRT [36]. Then, non-brain voxels were removed using BET [37], spatial smoothing (Gaussian kernel of FWHM 8.0 mm) was applied, and the entire 4D dataset was normalized using the grand-mean intensity. High pass temporal filtering (sigma = 50 s) was applied to restrict for task-related temporal patterns, and 4D sets were finally registered to the MNI152 template using FLIRT [38]. After this preprocessing, fMRI analysis of the task was carried out using Tensorial Independent Component Analysis (TICA) [39] as implemented in MELODIC, part of FSL. MELODIC allows fMRI data to be broken down into three-dimensional sets of vectors which describe signal variation across the temporal domain (time-courses), the spatial domain (spatial maps), and the subject domain (subject modes). Spatial maps include regions of synchronous activations and deactivations, and subject modes reveal the strength of both these activations and deactivations; higher subject modes values indicate higher activations and higher deactivations of the positive and negative parts of an IC respectively. A simple Pearson correlation was performed on the rank-1 estimated time course and the task time-series model, in order to identify task-related components. Spatial maps of the IC of interest were thresholded using a Gaussian/gamma-mixture model and represented on the MNI standard template.
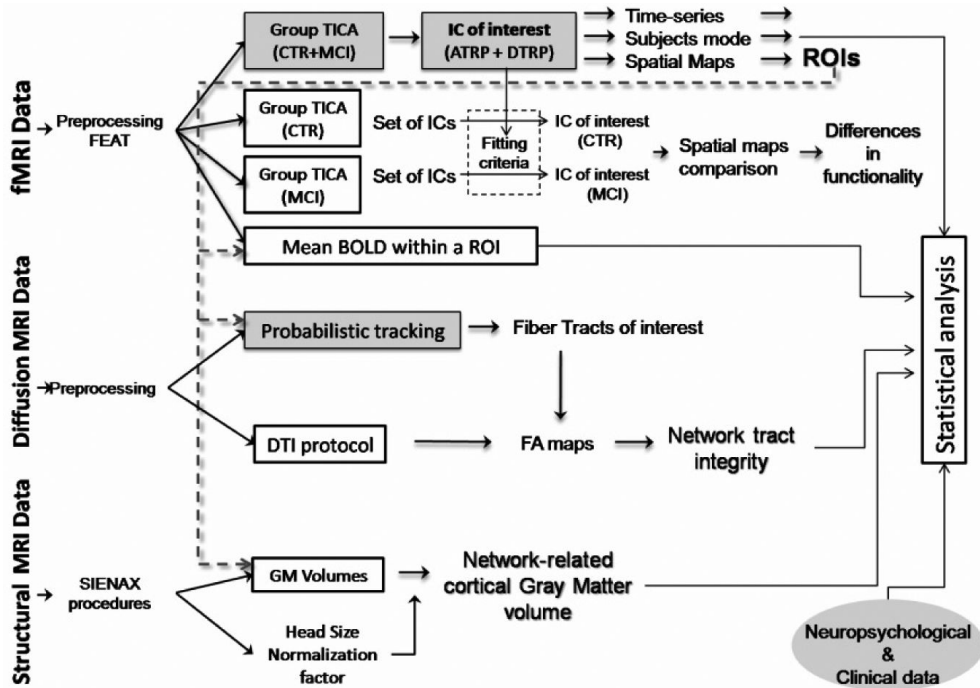
Fig. 2. Multi-modal MRI processing and analysis stream.

As shown in Fig. 2, group-TICA decompositions were performed at two levels. The first decomposition included data for all the subjects, with the specific aim of finding a common task-related region. Then, a second analysis was performed separately for the two groups (HE and MCI) in order to evaluate differences in the spatial extent of the network.

The main task-related component was selected from the whole-group analysis, using information from both time-series analysis and subject modes. Then, to select the analog component in the separate ICAs, we used the spatial cross correlation value (fslcc in FSL).

The ROI definition process was derived from the thresholded spatial map of the selected component. Large (i.e., more than 50 voxels) isolated clusters in GM regions were separated into binary ROIs.

Finally, from the preprocessed fMRI data, a measure of the mean BOLD activity within the defined ROIs was extracted separately for each individual and each condition (i.e., task, control and fixation).

Structural MRI analysis

Structural 3D-MPRAGE images were used to obtain GM volumes. Brain tissue volume, normalized for subject head size, was estimated with SIENAX [40]. In the first part of the SIENAX procedure, a volumetric scaling factor, which referred to the relationship be-

tween the subject's head size and the MNI152 standard template, was obtained for each subject. Next, tissue-type segmentation with partial volume estimation was carried out [41]. ROI GM volumes were extracted from the tissue-type segmentation. More specifically, each subject's GM volume was masked using the pre-defined binary ROIs (from functional activation maps) and the resulting volumes were calculated. Finally they were normalized using the scaling factor, to account for head-size differences. A voxel based morphometry (VBM) analysis was also performed on the GM maps, using tools available in FSL.

Diffusion MRI analysis

Diffusion MRI Images were analyzed using FDT (FMRIB's Diffusion Toolbox), a software tool for analysis of diffusion weighted images included in FSL [42–44]. First, data were corrected for distortions caused by the eddy currents in the gradient coils and for simple head motion, using the B0 non-diffusion data as a reference volume. Then, Fractional Anisotropy (FA) maps from each subject were obtained using a Diffusion Tensor Model fit. A probabilistic tractography algorithm was also applied to the diffusion images. For this purpose, in the first step, diffusion parameters were estimated using the BEDPOSTX tool from FSL, which computes a Bayesian estimation of the pa-

Table 1
Sample demographics and cognitive characteristics

	HE	a-MCI	t-test	p value
Age	75.20 (5.76)	74.33 (6.99)	0.91	0.37
Gender (women/men)	10/5	10/5	–	–
MMSE	27.67 (1.49)	25.50 (2.10)	3.31	< 0.001
Education (years)	8.93 (4.6)	8.87 (4.0)	0.04	0.97
Memory functions				
Recall of Constructional Praxis CERAD	8.13 (2.10)	4.73 (2.40)	4.12	< 0.0001
Free recall (FCSRT)	25.67 (5.76)	9.73 (5.21)	7.93	< 0.0001
Long term retrieval (FCSRT)	8.47 (1.99)	0.60 (1.12)	13.3	< 0.0001
Frontal functions				
Digit span (Inverse) (WAIS-III)	5.13 (1.88)	4.40 (1.68)	1.12	0.27
Symbol search (WAIS-III)	24.13 (10.09)	17.33 (5.51)	2.28	0.03
COWAT	24.80 (9.52)	23.53 (8.37)	0.38	0.70
Similarities (WAIS-III)	15.27 (4.57)	13.47 (3.46)	1.21	0.23
Language				
BNT	49.93 (5.39)	48.73 (4.26)	0.67	0.50
BDAE comprehension	14.93 (0.25)	14.87 (0.35)	0.59	0.55
Visuoperceptive / visuospatial functions				
Incomplete Letters VOSP	19.60 (1.92)	19.47 (0.92)	0.24	0.81
Number location VOSP	9.60 (0.63)	8.87 (1.64)	1.61	0.12
PDT score	14.07 (0.96)	13.60 (0.74)	1.49	0.15
Praxis				
Ideomotor praxis	5 (0)	5.40 (1.54)	1.00	0.32
Constructional praxis CERAD	9.47 (1.64)	9.60 (1.63)	2.22	0.82

HE: healthy elders, a-MCI: amnestic Mild Cognitive Impairment. MMSE: Mini-Mental State Examination. CERAD: Consortium to Establish a Registry for Alzheimer's Disease: Clinical and Neuropsychology Assessment. FCRST: Free and cued selective reminding test. VOSP: Visual Object and Space Perception Battery. PDT: Perception Digital Test. WAIS-III: Wechsler Adult Intelligence Scale III version. COWAT: Controlled Oral Word Association Test. BNT: Boston Naming Test. BDAE: Boston Diagnostic Aphasia Battery.

rameters (i.e., diffusion parameters and local fiber directions) using sampling techniques and a model of Crossing Fibers [42]. The density functions obtained were subsequently used to estimate connectivity between pairs of ROIs (seed ROI and end ROI) with the PROBTRACX tool from FSL. The entire probabilistic tracking procedure was carried out in each subject's anatomical space. Using the probabilistic tractography algorithm, we obtained individual maps for each pair of ROIs, where each voxel value indicated the probability of having fibers connecting the two regions. These maps were thresholded (at 2% of their maximum) in order to remove very-low probability fiber paths. Finally, the pathways obtained were visually inspected. Individual FA scores inside each pathway were then used to quantify and compare the integrity of the paths identified (Fig. 2).

Statistical analyses

Functional measurements (mean BOLD signal within each ROI and condition), ROI GM volumes and tract integrity (mean FA along the tracts-of interest) were introduced into SPSS v.16 (Statistical Package for Social Sciences, Chicago, II, USA). Between groups comparison were performed using two-tailed t-tests. Partial correlations were also undertaken to investigate the relationship between functional and structural components of the network and the relationship with cognitive performance within each group. In the partial correlation analysis, age, gender, and task performance (when not evaluated) were included as covariates. Results were considered as statistically significant if they attained a p value < 0.05. When the analyses included multiple comparisons, Bonferroni correction was applied.

RESULTS

Table 1 summarizes the main characteristics of the sample groups, including demographic variables and cognitive measures. HE and a-MCI patients were comparable in age, gender distribution, global cognitive performance, language, and visuoperceptive-visuospatial functions. Educational levels were also similar between groups. In general, attentional/frontal lobe functions were also comparable, except for the Symbol Search test assessing speed of processing and working memory. Despite the statistical differences that
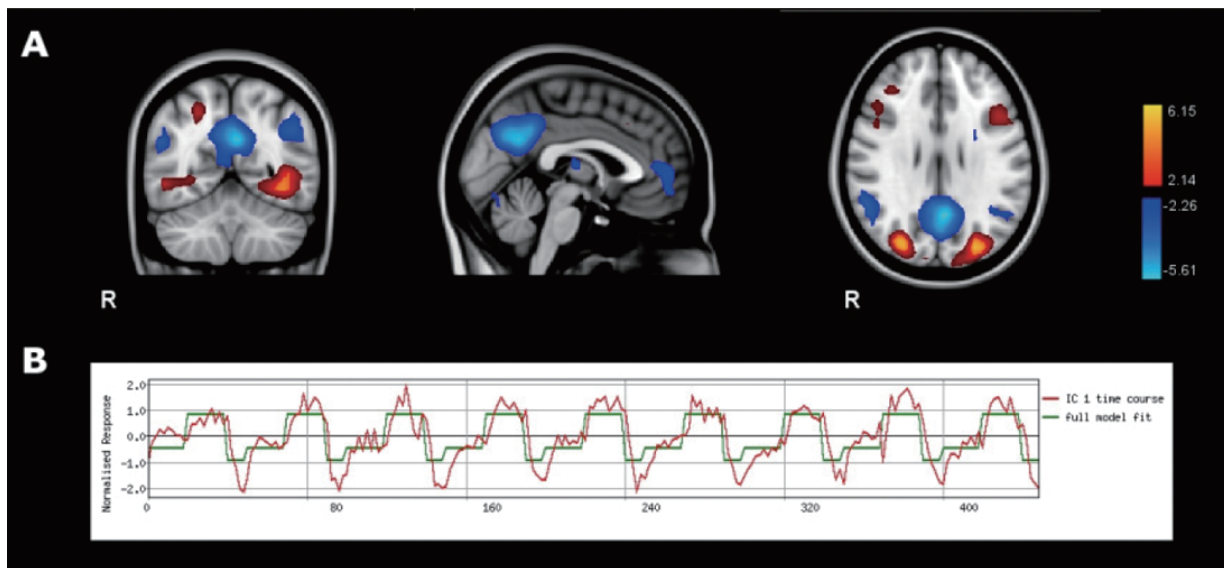
Fig. 3. Spatial maps (A) and time-course (B) of the main task-related component obtained from the whole group (HE and a-MCI subjects) TICA analysis. In (A), regions in red-yellow show the positive part of the component (task-activations) and regions in blue are the negative part (task-deactivations or rest-activations). In (B), red line shows the rank-1 approximation of the IC's temporal activation, and green line shows an idealized reference function of the task.

emerged for this test between groups, none of the patients was clinically impaired in any of the above cognitive domains when analyzed individually. As expected, patients performed worse on both verbal and visual episodic memory tests. Task performance scores (correct responses and response times) inside the scanner were lost for a high number of subjects ($n = 6$) due to technical problems. Therefore, the score on the clinical test administered to the subjects before the MRI session was used in all cases to measure individual performance.

Functional networks identified

The main task-related component was selected from the group T-ICA decomposition, including all the subjects (HE and a-MCI). Its time course fitted the task time series with Pearson's $r = 0.72$ ($p < 0.001$) and its fMRI signal was specific for the task scans ($t = 15.92$, $p < 0.001$ in the blurred images > colored squares contrast). Other task-related components were found, but they were not considered in this study either because (i) they were not homogeneous throughout the whole sample (with very high subject modes in a few subjects, and very low or negative values in the others) or (ii) they did not form a consistent anatomical network (i.e., isolated regions located in the non-GM brain region).

This main task-related pattern comprised ATRP (Fig. 3A, red-yellow maps) and DTRP (Fig. 3A, blue maps). The ATRP included areas whose activity was synchronously higher in the task scans (i.e., blurred images) and concomitantly lower in the control stimulus (i.e., square colours) or even lower in rest scans (Fig. 3B, red line). Conversely, regions in the DTRP were strongly deactivated during the task scans, with medium levels in the control scans and no deactivation at rest. The ATRP network included anterior and posterior areas of both hemispheres, with the posterior parts of the right hemisphere being the most clearly represented. In posterior regions, the ATRP was formed bilaterally by parts of the primary (BA17) and secondary associative visual areas (BA18, BA19), temporoccipital, and parietal regions. Ventrally, the posterior segments of the lingual and fusiform cortices (BA 18/19) were involved bilaterally, as was the inferior temporal gyrus (BA37). Dorsally and in the medial aspect of the occipital lobe, the cuneus (BA18/31) was also included in the ATRP network, as well as the superior occipital gyrus (BA19) bilaterally. Close to this latter region and in the right hemisphere, parts of the inferior (gyrus angularis BA39) and superior parietal lobe (BA7) were also included. In frontal regions the inferior and middle frontal gyri were involved (BA 44/45, 6 and 9). In the right hemisphere the functional network also included parts of the BA6 corresponding to the precentral gyrus.
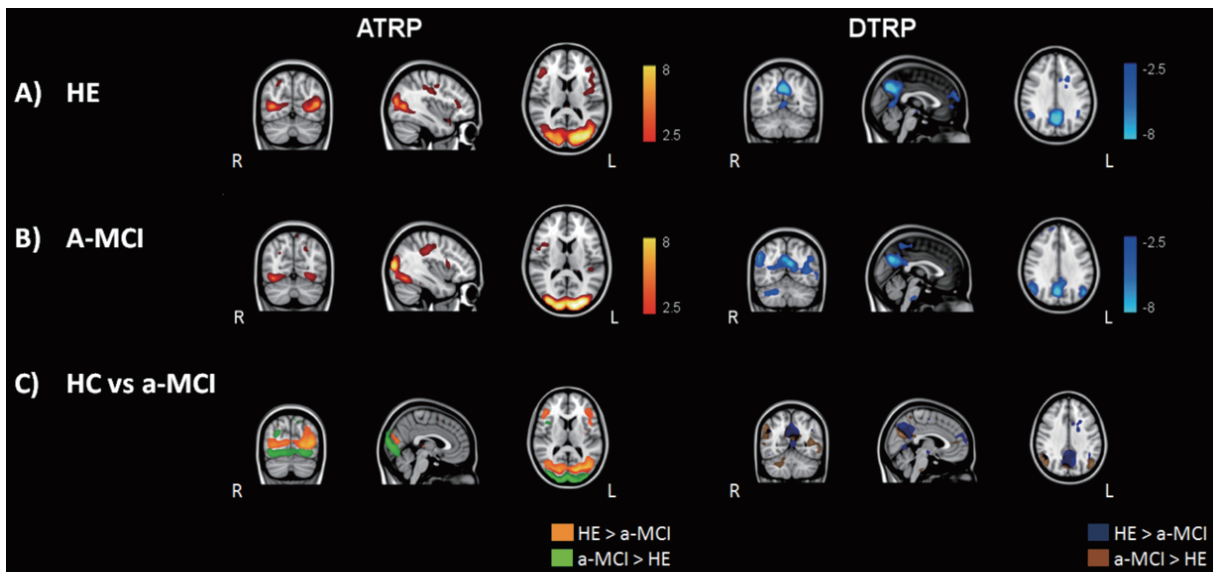
Fig. 4. Spatial Maps for the ATRP and DTRP corresponding to the main task-related component for the HE group (A) and the a-MCI group (B), and inferences between these maps (C).

The DTRP included medial and lateral cortical regions in close correspondence with those described as the DMN [25,27]. In medial prefrontal cortex regions, the anterior cingulate was involved (BA24 and BA32). In posterior areas the middle occipital (BA31) and parietal (BA7) precuneus, the posterior cingulate cortex (PCC, BA31, and BA23) and the retrosplenial cingulate cortex (BA29/30) were included. Finally, regions of the inferior parietal lobe (BA39 and BA40 of both hemispheres), and regions of the right superior temporal gyrus (BA41) also formed part of this network (see Figs 3 and 5).

fMRI differences of the main task-related network between HE and a-MCI patients

When HE and MCI groups were analyzed in separate ICAs, we found differences regarding the spatial extension of the main task-related component for both groups (see Methods for the procedures used in the selection of the component). Figure 4 shows the task-related component for each group (Fig. 4A and 4B) and inferences between them (Fig. 4C). For ease of presentation, activation and deactivation regions from a single IC were split into separate figures. Here we see that the spatial map of the ATRP comprised occipital regions that were more ventrally orientated in the MCI group than in HE. The differential areas were found in the middle occipital gyrus, fusiform, and lingual cortices (BA17/18/19), with the occipital fusiform cortex being the region that showed the largest differences between groups, extending to the anterior fusiform (temporal) among MCI. In contrast, among HE, increased activity was found in the cuneal cortex, the middle occipital gyrus (BA19), and the inferior (BA39) and superior parietal lobe (BA7). Finally, in anterior regions we found a large cluster of increased activation among HE in the inferior frontal gyrus (BA6/BA46). However, in nearby areas a-MCI also exhibited a stronger fMRI signal (inferior frontal gyrus and precentral gyrus (BA6/9). Smaller clusters of differences were further observed in the orbital cortex (BA13/BA47) where HE showed increased activations, and in the postcentral, and precentral sulcus (BA2/3/4), subgenual cortex (BA25/32) and frontal pole, where the fMRI signal was higher in a-MCI than in HE.

The spatial extension of the DTRP also differed between groups. First, the posteromedial area was larger for the HC group in the precuneus (BA7) and PPC (BA31 and BA 29/30) cortices. Conversely, in a-MCI the extension was bigger in inferior parietal lobes including the angular gyrus (BA39) bilaterally and the supramarginal gyri in the right hemisphere (BA40).

Gray matter volumes within the identified functional networks

Several ROIs were defined on the basis of the functional results reported (see Methods and Fig. 2 for the methodology used). First, four isolated regions were
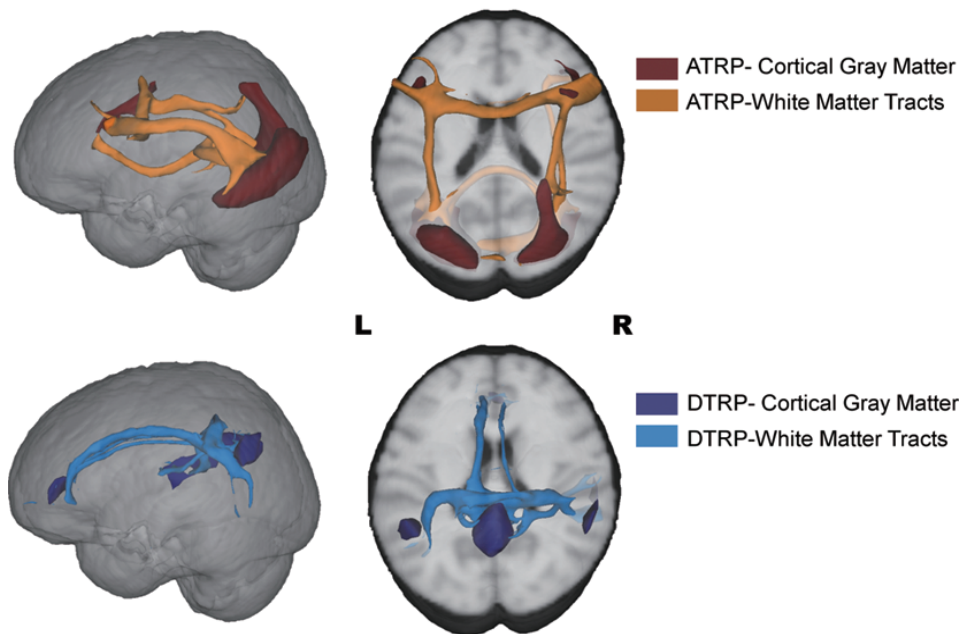
Fig. 5. Three dimensional representation of the structural brain network subserving the main task-related ICA pattern in healthy elders and a-MCI patients. A complete description of all the cortical areas and WM connectivity paths shown in the figure is given in the main text.

identified within the ATRP, two in posterior brain areas (posterior right and posterior left) and two in the anterior part (anterior right and anterior left). Furthermore, three ROIs were defined from DTRP areas (henceforth the anterior cingulate ROI, posteromedial ROI, and bilateral inferior parietal ROIs). Note that in the case of the DTRP, the two inferior parietal regions (bilaterally) were considered as a single ROI.

GM volumes were measured within each ROI. Group differences are shown in Table 2 and Fig. 7. GM volumes in areas of the DTRP showed statistically significant differences, mainly due to differences in the posteromedial ROI (precuneus/PCC).

Moreover, a standard whole-brain VBM analysis was also performed to compare GM from both groups. Results from this analysis are not shown, but they corroborated the previous literature on MCI patients (being the main differences in regions in the temporal lobes, such as the hippocampus and parahippocampus, lingual gyrus, and temporal fusiform, $p < 0.01$, FWE corrected).

White matter connectivity

WM fiber tracts were identified using probabilistic tractography as described previously. Results can be seen in Figs 5 and 6. Figure 5 contains a three-dimensional representation of cortical areas and fiber pathways connecting them (pathways are averaged across all the subjects). In Fig. 6, average connectivity maps for each group are represented separately on an FA template.

In the ATRP, fronto-occipital connectivity was analyzed separately for each hemisphere (using its posterior ROI and anterior ROI as seed regions), and inter-hemispheric connectivity was analyzed between both the two anterior and the two posterior ROIs. Fiber tracking results indicated that the main paths connecting ATRP regions were the superior longitudinal fasciculus bilaterally, the right inferior longitudinal fasciculus, and the right inferior fronto-occipital fasciculus. Moreover, the splenium and the genu of the corpus callosum provided inter-hemispheric connectivity.

As regards the identification of WM fiber tracts connecting DTRP areas, the cingulum bundle bilaterally was clearly identified as the major component connecting the posteromedial ROI with the anterior cingulate. Furthermore, DTRP-related structural connectivity was also found in the right inferior fronto-occipital fasciculus, the inferior longitudinal fasciculus bilaterally and, finally, in the splenium of the corpus callosum connecting posteromedial and bilateral inferior parietal ROIs.

Moreover, FA values were used to quantify fiber integrity within each pathway. Comparisons of these

Table 2
GM and FA measurements within the ATRP and DTRP areas

|	HE	a-MCI	t-test	p value
ATRP measures				
GM volumes (mm^3)	31564 (2876)	29576 (3627)	1.70	0.11
Left posterior areas	15894 (1720)	14816 (1970)	1.59	0.12
Left anterior areas	1581 (125)	1523 (160)	1.09	0.28
Right posterior areas	11343 (1306)	10596 (1610)	1.39	0.17
Right anterior areas	2746 (304)	2639 (257)	1.04	0.31
FA scores				
Left longitudinal tracts	0.445 (0.038)	0.427 (0.041)	1.23	0.22
Right longitudinal tracts	0.410 (0.031)	0.386 (0.031)	2.07	0.05
Anterior CC	0.399 (0.084)	0.391 (0.037)	0.35	0.73
Posterior CC	0.460 (0.057)	0.439 (0.067)	0.92	0.36
DTRP measures				
GM volumes (mm^3)	15240 (1079)	14112 (1564)	2.30	0.03
Posteromedial area	6897 (649)	6195 (1050)	2.20	0.04
Bilateral parietal areas	6477 (710)	6059 (783)	1.52	0.13
Anterior cingulate	1891 (203)	1797 (216)	0.61	0.55
FA scores	0.387 (0.032)	0.362 (0.029)	2.56	0.016
Cingulum bundle	0.396 (0.032)	0.369 (0.025)	2.54	0.017
Posterior interhemispheric tracts	0.397 (0.038)	0.371 (0.034)	2.0	0.06
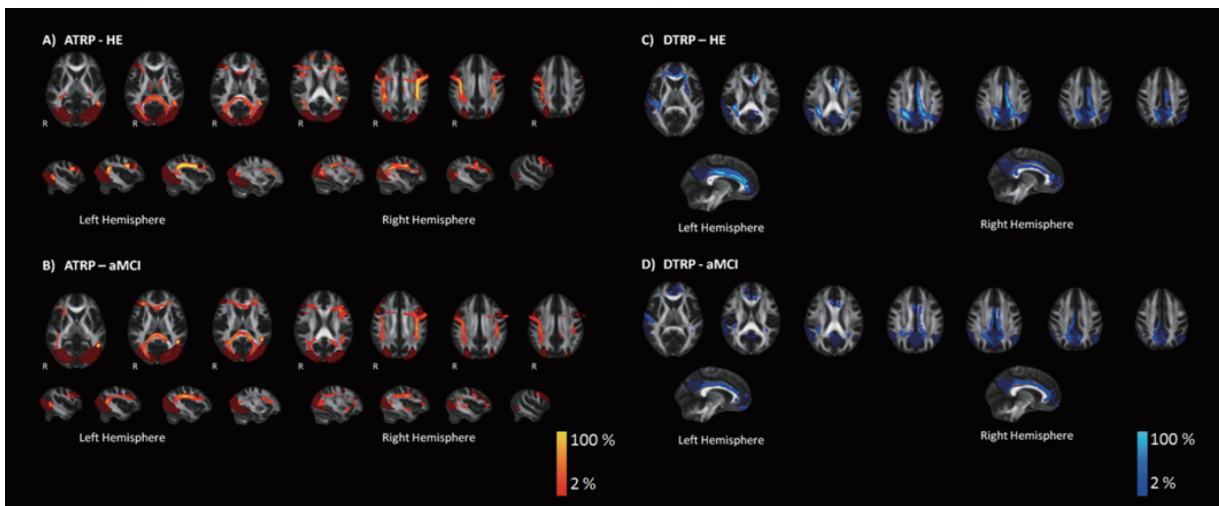
Fig. 6. Mean probabilistic maps reflecting WM connectivity in both ATRP (A and B) and DTRP (C and D) and for the two groups (HE and a-MCI) separately.

results showed significant differences between groups only in DTRP related pathways, due mainly to differences in the tracts of the cingulum bundle (see Table 2 and Fig. 7).

Correlations between structural measures, functional activation, and task performance

Task/rest activations

As expected, there was a high correlation between the mean BOLD signal in ATRP regions during task performance and in DTRP regions during rest periods for the HE and a-MCI groups ($r = 0.83$, $p < 0.001$).

Activation and task performance

Mean BOLD signal measured in the posteromedial ROI of the DTRP during rest (rest-DTRP activation) correlated positively with task performance only in the HE group ($r = 0.72$, $p = 0.03$, corrected). No relationships with the PDT score and task-ATRP activations or rest-DTRP activation were found in the a-MCI group.

Structure and task performance

No relationships were found in the HE group between main task-related pattern structural measures and task performance. Moreover, for the a-MCI group, two significant correlations were found, both concerning
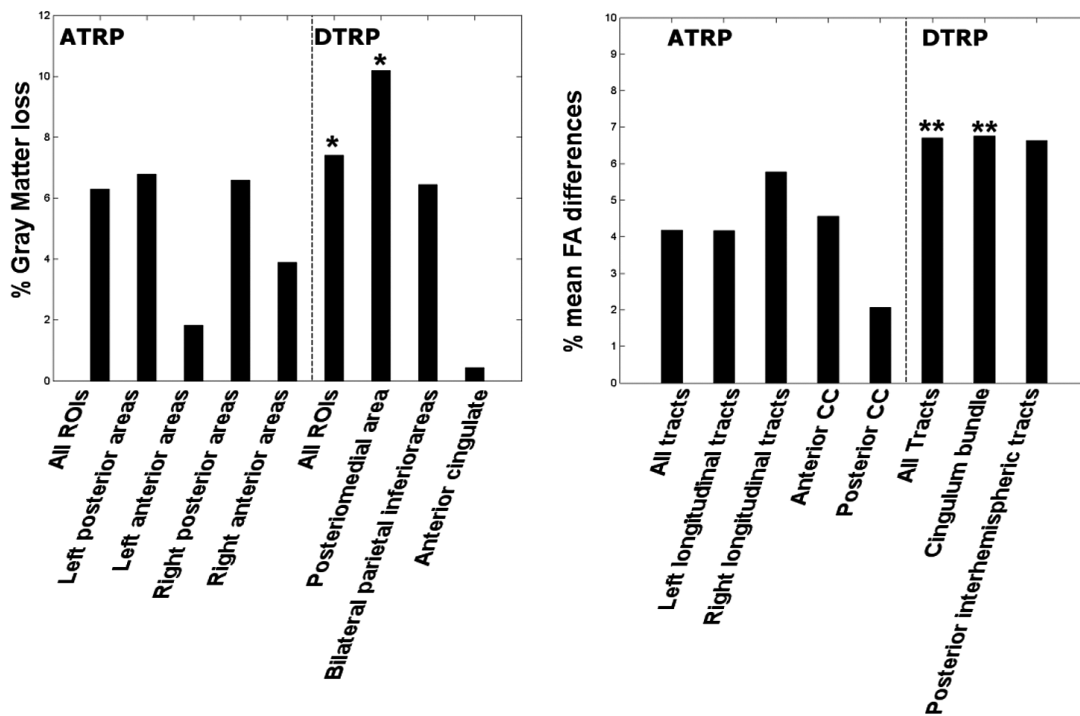
Fig. 7. Percentages of mean GM and tract-related FA loss for the MCI group relative to the HE group. An extended description of the anatomical cortical regions included in each ROI, and fiber tracts considered in each connectivity pathway is given in the main text. $^*p < 0.05$ in the HC vs. a-MCI t-test, and $^{**}p < 0.02$ in the HC versus a-MCI t-test.

DTRP-related measures. Task performance correlated positively with both DTRP GM volumes ($r = 0.60$, $p = 0.04$, uncorrected) and mean FA within the longitudinal medial tracts of the DTRP ($r = 0.62$, $p = 0.03$, uncorrected). However, these two latter results did not survive correction for multiple comparisons.

Function and structure

When the mean BOLD signal was measured individually in all the ROIs defined, only the signal measured in the two ROIs formed by bilateral parietal regions of the DTRP (BA 39/40) showed negative correlations with its underlying GM volumes in the a-MCI group ($r = -0.73$, $p = 0.011$).

Finally, some analyses considering the follow-up results were performed, a-MCI patients were divided into two groups, converters ($n = 5$) and no converters ($n = 10$). There were no differences between the two subgroups (converters versus no converters) in any of the measures found to be sensitive to differentiate between HE and a-MCI patients.

DISCUSSION

To our knowledge, this is the first MRI-based study in MCI patients to characterize the GM and WM anatomical components of a task related cognitive cerebral network. Several main findings emerge from our multimodal MRI study. First, the ICA analyses identified two major anatomic-functional networks in the main component related to the processing of the visual task. The ATRP was identified by virtue of higher activity mainly in occipital, temporal, and parietal areas, and to a lesser extent in frontal regions. Likewise, the DTRP comprised areas anatomically comparable to the DMN in which increased activity was observed during passive processing. In the ARTP network, a-MCI exhibited functional reorganizations reflected by an increase in the fMRI signal in ventral occipital areas compared to healthy elders in the context of comparable GM atrophy and WM fiber integrity. In DTRP regions, patients presented deactivation deficits in posteromedial areas and increased deactivation in lateral parietal regions. a-MCI patients showed GM atrophy in the regions underlying the DTRP network, particularly in the precuneus and PCC, as well as reduced WM integrity in struc-

tural pathways connecting DTRP areas, specifically in the cingulate bundles. Finally, relationships between structure, function and performance were found only in DTRP-related measures; in the HE group, activation of the PCC during rest was correlated with task performance, and among patients, the structural measures of the DTRP network correlated with task performance. Nonetheless, this latter result should be considered with caution, since it did not survive multiple comparison correction.

Our findings for the ATRP revealed that regions activated during the processing of complex visual pictures mainly span primary and lateral extrastriate regions, the posterior parts of the temporal lobes (temporo-occipital) and the superior and inferior parietal cortices. Overall, this pattern of activation is consistent with previous PET and fMRI studies of brain activity associated with face and object recognition, spatial localization [45–48], and visuospatial attention [49]. Hence, topographic analysis of the ATRP network suggests that our task incorporates both visuoperceptive components of the ventral visual stream (identification of the blurred images) and the visuospatial function related to the dorsal visual system (selecting the image in a given position in space). Moreover, and especially in the right hemisphere, areas of the dorsolateral prefrontal cortex including the inferior prefrontal (BA45) and dorsal premotor (BA6) cortices were also found to be part of the network. The involvement of these regions also corroborates the findings of Bokde et al. [20] in MCI patients using a visuoperceptive task and functional connectivity analyses, and those of Vannini et al. [18] who used a visuospatial task based on an angle discrimination test in MCI. In our study the observation of frontal lobe activity supports the idea that it includes both visual systems, as the prefrontal cortex is the principal area of integration of visual information from the ventral and dorsal pathways [50].

The probabilistic tractography analysis identified WM tracts connecting ATRP cortical sites compatible with anatomical descriptions of the superior longitudinal fasciculus dorsally and the inferior longitudinal and fronto-occipital fasciculi ventrally. In general, the identification of these major bundles corroborates a recent study in young healthy subjects which identified WM tracts based on fMRI activations during a visuospatial attention task [51]. The convergence between the two sets of findings provides methodological support for the idea that the pathways identified in our studies among HE and MCI correspond to the actual anatomical connections between dorsolateral and posterior functional

brain areas. The fact that in our study superior longitudinal fasciculi were identified bilaterally, whereas inferior longitudinal and inferior fronto-occipital fasciculi were only located in the right hemisphere, may suggest a stronger load of the task in the dorsal than in the ventral pathway.

Regarding group comparisons for the ATRP functionality, a-MCI showed higher activity than HE in more ventral cortices. Previous studies [22,52] have reported increased activations in AD in the fusiform gyrus during visuospatial processing and reduced activations in areas of the dorsal stream. These findings build on previous fMRI studies of visuospatial [18,19] and visuoperceptive [19,20] functions in MCI, showing that patients tend to use alternative networks during complex visual processing. One possible explanation may be that a-MCI patients use distinct functional strategies, as it has already been observed by Bokde et al. [22], Alternatively, the increased activation in ventral pathway may reflect the use of the same functional strategy as in HE (albeit used less efficiently) and the need to recruit additional resources as a compensatory mechanism. The neuropathological damage present in MCI [53–56] may account for the existence of these functional compensatory mechanisms. We also observed some differences in frontal lobe areas, including both increased and decreased activations. Increased activation would reveal compensatory mechanisms in anterior areas coexisting with compromised posterior systems [19]. In contrast, areas of decreased activation may reflect dysfunctional prefrontal regions characteristic of this condition, as previously shown in an fMRI study of executive functions [15]. Overall, the fMRI frontal lobe findings were relatively modest compared to the posterior regions and included increased and decreased activations; their interpretation is complex and cannot be completely elucidated in the present study.

Concerning the comparison of the anatomical components of the ATRP, GM volumes and fiber tract FA measures did not reveal significant differences between a-MCI and healthy elders. In our study, the morphological characteristics of the ATRP did not correlate with task performance or fMRI changes. However, as functional differences were found, these results are in line with previous fMRI reports that showed functional reorganizations preceding marked MRI-detectable brain atrophy, a finding already demonstrated in studies of at-risk dementia populations [6,57,58]. The lack of structure-function associations of our study is at variance with those of Teipel and colleagues [21] in MCI, who found relationship between brain activity and the

underlying GM volumes. The differences between the results are probably due to distinct methodological approaches (region-based vs. whole-brain analyses) and may also be related to different levels of task-demands. Furthermore, a study by Gold et al. [59] also reported differential fMRI patterns in the fusiform gyrus between a-MCI and healthy elders, accompanied by preserved underlying anatomy (but GM atrophy in the medial temporal lobe was observed in a whole-brain VBM analysis). In summary, although our study shows that a-MCI patients recruit a differential pattern of brain activity; these functional changes do not seem to correspond to clearly detectable damage in GM and WM regions of this network.

Using an ICA approach – a powerful tool to find spatio-temporally independent brain networks – we were able to identify, in addition to the main task-activation areas, the task-deactivation network which closely matched the anatomical regions of the DMN [25,26]. First, within this pattern, we observed a high correlation between rest-related activation and task performance in the HE group, which was in concordance with previous studies of DMN activity and its relationship with task outcome [60,61]. In contrast, such correlations could not be observed for the functional components of the ATRP in any of the studied groups. A plausible explanation is that the narrow range of score distributions for task performance precluded to observe covariations with BOLD variability in a brain network (ATRP) comprised of brain regions directly involved in high order visual processing, as all healthy elders (but also most patients) obtained high scores with low inter-individual variability. On the other hand, the associations regarding the posterior DMN could reflect either a system already affected by the ageing process [62] and/or a system that correlates with cognitive function in a more general way [27], and thus being more sensitive to a broader range of subtle behavioral differences. This relationship (DMN and task performance) was not found in a-MCI, probably due to the atrophy – in DTRP areas in this group. Furthermore, from the separate ICAs approach, in the DTRP network, a-MCI exhibited deficits mainly in posteromedial structures, including the PCC and the precuneus. These observations have been already reported in fMRI studies on memory tasks [13,28,63,64] and in resting-fMRI studies [30,65,66]. A further observation was that besides exhibiting disruption of posteromedial deactivations, the opposite pattern was observed in lateral inferior parietal areas. These latter findings are in agreement with those of Qi et al. [30], who reported areas of greater signal in parietal regions in the context of reduced PCC activity, and are also comparable with those of Bai et al. [66]. These neocortical activations have been associated to compensatory responses related to memory process. Our study also provides the direct observation that higher task-related deactivation in inferior parietal regions appears to be in response to greater GM atrophy, as negative correlations between GM volumes and brain activity were observed only for the a-MCI group in these particular regions.

The presence of both significant GM atrophy and reduced microstructural WM damage in DRTP regions in our patients was one of the principal findings of our investigation. To our knowledge, only two previous reports were specifically designed to investigate the relationship between structural changes and functional resting-state networks in a-MCI; these studies included VBM analyses and were restricted to GM measures [65, 66]. In one of those studies, GM atrophy in patients did not overlap with the functional resting networks identified, including the DMN [65]; however, they also found GM atrophy in the PPC/precuneus area. As discussed above, here DTRP structural alterations emerged in the context of an anatomically preserved main-task (i.e., ATRP) brain network. Furthermore, we observed a correlation between structural DTRP-related measures (GM volume and mean FA within the cingulum) and task performance, suggesting that structural alterations in the DMN already have an impact on cognitive variation in a-MCI. However, these latter results did not survive correction for multiple comparisons and thus need to be considered very cautiously. Taken together, these observations emphasize the need to consider not only the functionality but also the structure of the DMN-related regions as early markers of neurodegeneration in preclinical dementia, a notion that in general is compatible with the progressive convergence of functional, molecular and structural damage in this area in established AD patients reported by Buckner and colleagues [27,67]. More specifically, the clinical relevance of functional and structural alterations in these posteromedial regions in a-MCI has been reported in separate recent findings revealing focal GM atrophy in the posterior cingulate region (BA 29/30 and BA 23 retrosplenial cortex [68], as well as regional metabolic dysfunctions [69,70] and fMRI deactivation alterations [64] in a-MCI patients with confirmed conversion to dementia.

Finally, in our study we identified major WM fiber bundles connecting DTRP cortical areas. In spite of the methodological differences in DTI sequence ac-

quisition and processing, these results corroborate recent resting-state fMRI findings that the connectivity of functional networks including the DMN is generally supported by direct structural connectivity, as proven by the identification of the same main bundles, such as the cingulum [71,72], the superior fronto-occipital fasciculus, and the genu of the corpus callosum [73]. Anatomically, a-MCI patients showed significant FA reductions in medial tracts compatible with the anatomical characterization of the cingulate bundle. In our previous DTI study using a voxel-wise DTI analysis, we observed mean FA reductions among a-MCI in all regions where AD patients showed alterations, including parts of this pathway [74]. Thus, while the results are concordant, the focused damage reported here in this particular tract, but not the other damage identified in the present study, is probably due to a more thorough methodological approach involving the performance of probabilistic tractography rather than whole-brain voxel-wise analyses. Overall, cingulate bundle involvement based on FA measures has been demonstrated in recent DTI literature in MCI [75–79]. The novelty of our study, besides being one of the few investigations of MCI to include tractography, is that we demonstrate microstructural damage of this bundle and posterior GM-associated regions and do not isolate them on the basis of an anatomical label, but as part of the anatomy integrated within functional deactivation areas during task performance. In the present report, we used FA as a measure of WM integrity, as it has been widely used in the literature. However it should be noted that underlying this common definition there may be a number of neuropathological or neuroanatomical processes such as demielinization, axon density, axonal membrane integrity, wallerian degeneration or intravoxel coherence of fiber integration [74]. Furthermore, a full established clinical-anatomopathological model of FA changes is not available. Thus, the general interpretation of FA reductions as loss of WM integrity stated in our study should be considered in the light of the current partial knowledge, which may change in the near future.

Several limitations of the present study should be considered and improved in further research. First, the inclusion of an AD group would have been desirable to investigate the anatomo-functional changes of the network identified, as brain damage progresses from normal aging to a-MCI to established dementia. However, as we stated above, the focus of the investigation was to determine which structural and functional components of the network and their interactions were already altered in the a-MCI stage, and so we only included patients with normal performance on the PDT test, validated in the Spanish population [33]. For this reason we were unable to gather a group of AD patients with clearly preserved cognitive function in this domain. A second limitation concerns the behavioral variable used in the correlations between the structural and functional findings of our integrated networks. Due to technical problems, a significant proportion of responses obtained within the fMRI were lost and thus we were obliged to substitute them with the direct scores of the PDT test, for correlations with MRI data. Since our fMRI task was a direct adaptation of this test using the same stimuli, one would expect similar proportional performances in both tasks, but the actual direct correlations between responses recorded within the fMRI were not available. Finally, another limitation was that, besides having the follow-up information, the small number of subjects in the sample probably precluded to establish conclusions of how the parameters analyzed here could be helpful to determine conversion from MCI to AD.

In summary, the results of the present study provide novel information that should be useful for a better understanding of the functional and structural brain characteristics in MCI as a prodromal condition of AD. First, our study confirms previous findings indicating that the investigation of the visual system using fMRI provides useful information reflecting early changes in this condition. Importantly, they extend former knowledge demonstrating that brain dysfunctions, mainly in the dorsal pathway and probably reflecting compensatory mechanisms, can be evidenced at the stages where clinical compromise of visuoperceptive and visuospatial functions is excluded. This latter observation reinforces the idea that fMRI information may be considered as a potential biological marker of prodromal AD. Second, like some of the cortical areas of the visual system, the DMN especially in its posteromedial part exhibited functional abnormalities. Further, in our analytical approach from the fMRI information we were able to observe cortical atrophy as an anatomical substrate of these deactivation deficits. In the same comprehensive analyses, WM compromise was evidenced in the cingulate bundle, a main fiber pathway conforming part of the structural network of the DMN, as identified in previous studies. Thus, a second and most relevant implication derived from our study is that it supports the use of ICA-based, multimodal MRI investigation as a particularly sensitive approach to illuminate the breakdown of the anatomofunctional com-

ponents of the DMN in early AD, differentiating them from healthy aging. Finally it is also interesting to note at a practical level that since the cognitive task adapted to the fMRI was clinically spared in all patients, our multimodal study represents an heuristic approach to investigate the functional and structural status of relevant brain networks in prodromal stages of AD reducing common problems associated with complex tasks such as very poor execution levels, or inability to understand or perform the task in a proportion of patients.

ACKNOWLEDGMENTS

REFERENCES

[1] Petersen RC, Doody R, Kurz A, Mohs RC, Morris JC, Rabins PV, Ritchie K, Rossor M, Thal L, Winblad B (2001) Current concepts in mild cognitive impairment. *Arch Neurol* **58**, 1985-1992.

[2] Morris JC, Storandt M, Miller JP, McKeel DW, Price JL, Rubin EH, Berg L (2001) Mild cognitive impairment represents early-stage Alzheimer disease. *Arch Neurol* **58**, 397-405.

[3] Lopez OL, Kuller LH, Becker JT, Dulberg C, Sweet RA, Gach HM, Dekosky ST (2007) Incidence of dementia in mild cognitive impairment in the cardiovascular health study cognition study. *Arch Neurol* **64**, 416-420.

[4] Hampel H, Burger K, Teipel SJ, Bokde AL, Zetterberg H, Blennow K (2008) Core candidate neurochemical and imaging biomarkers of Alzheimer's disease. *Alzheimers Dement* **4**, 38-48.

[5] Ries ML, Carlsson CM, Rowley HA, Sager MA, Gleason CE, Asthana S, Johnson SC (2008) Magnetic resonance imaging characterization of brain structure and function in mild cognitive impairment: a review. *J Am Geriatr Soc* **56**, 920-934.

[6] Bookheimer SY, Strojwas MH, Cohen MS, Saunders AM, Pericak-Vance MA, Mazziotta JC, Small GW (2000) Patterns of brain activation in people at risk for Alzheimer's disease. *N Engl J Med* **343**, 450-456.

[7] Woodard JL, Seidenberg M, Nielson KA, Antuono P, Guidotti L, Durgerian S, Zhang Q, Lancaster M, Hantke N, Butts A, Rao SM (2009) Semantic memory activation in amnestic mild cognitive impairment. *Brain* **132**, 2068-2078.

[8] Bai F, Zhang Z, Watson DR, Yu H, Shi Y, Yuan Y, Zang Y, Zhu C, Qian Y (2009) Abnormal functional connectivity of hippocampus during episodic memory retrieval processing network in amnestic mild cognitive impairment. *Biol Psychiatry* **65**, 951-958.

[9] Dickerson BC, Salat DH, Bates JF, Atiya M, Killiany RJ, Greve DN, Dale AM, Stern CE, Blacker D, Albert MS, Sperling RA (2004) Medial temporal lobe function and structure in mild cognitive impairment. *Ann Neurol* **56**, 27-35.

[10] Dickerson BC, Salat DH, Greve DN, Chua EF, Rand-Giovannetti E, Rentz DM, Bertram L, Mullin K, Tanzi RE, Blacker D, Albert MS, Sperling RA (2005) Increased hippocampal activation in mild cognitive impairment compared to normal aging and AD. *Neurology* **65**, 404-411.

[11] Machulda MM, Ward HA, Borowski B, Gunter JL, Cha RH, O'Brien PC, Petersen RC, Boeve BF, Knopman D, Tang-Wai DF, Ivnik RJ, Smith GE, Tangalos EG, Jack CR, Jr (2003) Comparison of memory fMRI response among normal, MCI, and Alzheimer's patients. *Neurology* **61**, 500-506.

[12] Machulda MM, Senjem ML, Weigand SD, Smith GE, Ivnik RJ, Boeve BF, Knopman DS, Petersen RC, Jack CR (2009) Functional magnetic resonance imaging changes in amnestic and nonamnestic mild cognitive impairment during encoding and recognition tasks. *J Int Neuropsychol Soc* **15**, 372-382.

[13] Celone KA, Calhoun VD, Dickerson BC, Atri A, Chua EF, Miller SL, DePeau K, Rentz DM, Selkoe DJ, Blacker D, Albert MS, Sperling RA (2006) Alterations in memory networks in mild cognitive impairment and Alzheimer's disease: an independent component analysis. *J Neurosci* **26**, 10222-10231.

[14] Dannhauser TM, Walker Z, Stevens T, Lee L, Seal M, Shergill SS (2005) The functional anatomy of divided attention in amnestic mild cognitive impairment. *Brain* **128**, 1418-1427.

[15] Rosano C, Aizenstein HJ, Cochran JL, Saxton JA, De Kosky ST, Newman AB, Kuller LH, Lopez OL, Carter CS (2005) Event-related functional magnetic resonance imaging investigation of executive control in very old individuals with mild cognitive impairment. *Biol Psychiatry* **57**, 761-767.

[16] Bosch B, Bartres-Faz D, Rami L, Arenaza-Urquijo EM, Fernandez-Espejo D, Junque C, Sole-Padulles C, Sanchez-Valle R, Bargallo N, Falcon C, Molinuevo JL (2010) Cognitive reserve modulates task-induced activations and deactivations in healthy elders, amnestic mild cognitive impairment and mild Alzheimer's disease. *Cortex* **46**, 451-461.

[17] Lenzi D, Serra L, Perri R, Pantano P, Lenzi GL, Paulesu E, Caltagirone C, Bozzali M, Macaluso E (2009) Single domain amnestic MCI: A multiple cognitive domains fMRI investigation. *Neurobiol Aging*, in press.

[18] Vannini P, Almkvist O, Dierks T, Lehmann C, Wahlund LO (2007) Reduced neuronal efficacy in progressive mild cognitive impairment: a prospective fMRI study on visuospatial processing. *Psychiatry Res* **156**, 43-57.

[19] Bokde AL, Lopez-Bayo P, Born C, Dong W, Meindl T, Leinsinger G, Teipel SJ, Faltraco F, Reiser M, Moller HJ, Hampel H (2008) Functional abnormalities of the visual processing system in subjects with mild cognitive impairment: an fMRI study. *Psychiatry Res* **163**, 248-259.

[20] Bokde AL, Lopez-Bayo P, Meindl T, Pechler S, Born C, Faltraco F, Teipel SJ, Moller HJ, Hampel H (2006) Functional connectivity of the fusiform gyrus during a face-matching task in subjects with mild cognitive impairment. *Brain* **129**, 1113-1124.

[21] Teipel SJ, Bokde AL, Born C, Meindl T, Reiser M, Moller HJ, Hampel H (2007) Morphological substrate of face matching in healthy ageing and mild cognitive impairment: a combined MRI-fMRI study. *Brain* **130**, 1745-1758.

[22] Bokde AL, Lopez-Bayo P, Born C, Ewers M, Meindl T, Teipel SJ, Faltraco F, Reiser MF, Moller HJ, Hampel H (2010) Alzheimer disease: functional abnormalities in the dorsal visual pathway. *Radiology* **254**, 219-226.

[23] Bokde AL, Ewers M, Hampel H (2009) Assessing neuronal networks: Understanding Alzheimer's disease. *Prog Neurobiol* **89**, 125-133.

[24] Shulman GL, Corbetta M, Buckner RL, Raichle ME, Fiez JA, Miezin FM, Petersen SE (1997) Top-down modulation of early sensory cortex. *Cereb Cortex* **7**, 193-206.

[25] Raichle ME, MacLeod AM, Snyder AZ, Powers WJ, Gusnard DA, Shulman GL (2001) A default mode of brain function. *Proc Natl Acad Sci U S A* **98**, 676-682.

[26] Greicius MD, Krasnow B, Reiss AL, Menon V (2003) Functional connectivity in the resting brain: a network analysis of the default mode hypothesis. *Proc Natl Acad Sci U S A* **100**, 253-258.

[27] Buckner RL, Andrews-Hanna JR, Schacter DL (2008) The brain's default network: anatomy, function, and relevance to disease. *Ann N Y Acad Sci* **1124**, 1-38.

[28] Pihlajamaki M, DePeau KM, Blacker D, Sperling RA (2008) Impaired medial temporal repetition suppression is related to failure of parietal deactivation in Alzheimer disease. *Am J Geriatr Psychiatry* **16**, 283-292.

[29] Rombouts SA, Damoiseaux JS, Goekoop R, Barkhof F, Scheltens P, Smith SM, Beckmann CF (2009) Model-free group analysis shows altered BOLD FMRI networks in dementia. *Hum Brain Mapp* **30**, 256-266.

[30] Qi Z, Wu X, Wang Z, Zhang N, Dong H, Yao L, Li K (2010) Impairment and compensation coexist in amnestic MCI default mode network. *Neuroimage* **50**, 48-55.

[31] Pfeffer RI, Kurosaki TT, Harrah CH, Jr, Chance JM, Filos S (1982) Measurement of functional activities in older adults in the community. *J Gerontol* **37**, 323-329.

[32] Warrington EK and James M (1991) A new test of object decision: 2D silhouettes featuring a minimal view. *Cortex* **27**, 370-383.

[33] Rami L, Serradell M, Bosch B, Villar A, Molinuevo JL (2007) Perception Digital Test (PDT) for the assessment of incipient visual disorder in initial Alzheimer's disease. *Neurologia* **22**, 342-347.

[34] Fazekas F, Chawluk JB, Alavi A, Hurtig HI, Zimmerman RA (1987) MR signal abnormalities at 1.5 T in Alzheimer's dementia and normal aging. *AJR Am J Roentgenol* **149**, 351-356.

[35] Smith SM, Jenkinson M, Woolrich MW, Beckmann CF, Behrens TE, Johansen-Berg H, Bannister PR, De Luca M, Drobnjak I, Flitney DE, Niazy RK, Saunders J, Vickers J, Zhang Y, De Stefano N, Brady JM, Matthews PM (2004) Advances in functional and structural MR image analysis and implementation as FSL. *Neuroimage* **23 Suppl 1**, S208-S219.

[36] Jenkinson M, Bannister P, Brady M, Smith S (2002) Improved optimization for the robust and accurate linear registration and motion correction of brain images. *Neuroimage* **17**, 825-841.

[37] Smith SM (2002) Fast robust automated brain extraction. *Hum Brain Mapp* **17**, 143-155.

[38] Jenkinson M and Smith S (2001) A global optimisation method for robust affine registration of brain images. *Med Image Anal* **5**, 143-156.

[39] Beckmann CF and Smith SM (2005) Tensorial extensions of independent component analysis for multisubject FMRI analysis. *Neuroimage* **25**, 294-311.

[40] Smith SM, De Stefano N, Jenkinson M, Matthews PM (2001) Normalized accurate measurement of longitudinal brain change. *J Comput Assist Tomogr* **25**, 466-475.

[41] Zhang Y, Brady M, Smith S (2001) Segmentation of brain MR images through a hidden Markov random field model and the expectation-maximization algorithm. *IEEE Trans Med Imaging* **20**, 45-57.

[42] Behrens TE, Berg HJ, Jbabdi S, Rushworth MF, Woolrich MW (2007) Probabilistic diffusion tractography with multiple fibre orientations: What can we gain? *Neuroimage* **34**, 144-155.

[43] Behrens TE, Johansen-Berg H, Woolrich MW, Smith SM, Wheeler-Kingshott CA, Boulby PA, Barker GJ, Sillery EL, Sheehan K, Ciccarelli O, Thompson AJ, Brady JM, Matthews PM (2003) Non-invasive mapping of connections between human thalamus and cortex using diffusion imaging. *Nat Neurosci* **6**, 750-757.

[44] Behrens TE, Woolrich MW, Jenkinson M, Johansen-Berg H, Nunes RG, Clare S, Matthews PM, Brady JM, Smith SM (2003) Characterization and propagation of uncertainty in diffusion-weighted MR imaging. *Magn Reson Med* **50**, 1077-1088.

[45] Haxby JV, Grady CL, Horwitz B, Ungerleider LG, Mishkin M, Carson RE, Herscovitch P, Schapiro MB, Rapoport SI (1991) Dissociation of object and spatial visual processing pathways in human extrastriate cortex. *Proc Natl Acad Sci U S A* **88**, 1621-1625.

[46] Haxby JV, Horwitz B, Ungerleider LG, Maisog JM, Pietrini P, Grady CL (1994) The functional organization of human extrastriate cortex: a PET-rCBF study of selective attention to faces and locations. *J Neurosci* **14**, 6336-6353.

[47] Clark VP, Keil K, Maisog JM, Courtney S, Ungerleider LG, Haxby JV (1996) Functional magnetic resonance imaging of human visual cortex during face matching: a comparison with positron emission tomography. *Neuroimage* **4**, 1-15.

[48] Grill-Spector K (2003) The neural basis of object perception. *Curr Opin Neurobiol* **13**, 159-166.

[49] Corbetta M, Miezin FM, Shulman GL, Petersen SE (1993) A PET study of visuospatial attention. *J Neurosci* **13**, 1202-1226.

[50] Ungerleider LG, Courtney SM, Haxby JV (1998) A neural system for human visual working memory. *Proc Natl Acad Sci U S A* **95**, 883-890.

[51] Umarova RM, Saur D, Schnell S, Kaller CP, Vry MS, Glauche V, Rijntjes M, Hennig J, Kiselev V, Weiller C (2010) Structural connectivity for visuospatial attention: significance of ventral pathways. *Cereb Cortex* **20**, 121-129.

[52] Prvulovic D, Hubl D, Sack AT, Melillo L, Maurer K, Frolich L, Lanfermann H, Zanella FE, Goebel R, Linden DE, Dierks T (2002) Functional imaging of visuospatial processing in Alzheimer's disease. *Neuroimage* **17**, 1403-1414.

[53] Markesbery WR, Schmitt FA, Kryscio RJ, Davis DG, Smith CD, Wekstein DR (2006) Neuropathologic substrate of mild cognitive impairment. *Arch Neurol* **63**, 38-46.

[54] Bennett DA, Schneider JA, Bienias JL, Evans DA, Wilson RS (2005) Mild cognitive impairment is related to Alzheimer disease pathology and cerebral infarctions. *Neurology* **64**, 834-841.

[55] Saito Y and Murayama S (2007) Neuropathology of mild cognitive impairment. *Neuropathology* **27**, 578-584.

[56] Schneider JA, Arvanitakis Z, Leurgans SE, Bennett DA (2009) The neuropathology of probable Alzheimer disease and mild cognitive impairment. *Ann Neurol* **66**, 200-208.

[57] Smith CD, Andersen AH, Kryscio RJ, Schmitt FA, Kindy MS, Blonder LX, Avison MJ (1999) Altered brain activation in cognitively intact individuals at high risk for Alzheimer's disease. *Neurology* **53**, 1391-1396.

[58] Bartres-Faz D, Serra-Grabulosa JM, Sun FT, Sole-Padulles C, Rami L, Molinuevo JL, Bosch B, Mercader JM, Bargallo N, Falcon C, Vendrell P, Junque C, D'Esposito M (2008) Functional connectivity of the hippocampus in elderly with mild memory dysfunction carrying the APOE epsilon4 allele. *Neurobiol Aging* **29**, 1644-1653.

[59] Gold BT, Jiang Y, Jicha GA, Smith CD (2010) Functional response in ventral temporal cortex differentiates mild cognitive impairment from normal aging. *Hum Brain Mapp* **31**, 1249-1259.

[60] Persson J, Lustig C, Nelson JK, Reuter-Lorenz PA (2007) Age differences in deactivation: a link to cognitive control? *J Cogn Neurosci* **19**, 1021-1032.

[61] Park DC, Polk TA, Hebrank AC, Jenkins LJ (2010) Age differences in default mode activity on easy and difficult spatial judgment tasks. *Front Hum Neurosci* **3**, 75.

[62] Damoiseaux JS, Greicius MD (2009) Greater than the sum of its parts: a review of studies combining structural connectivity and resting-state functional connectivity. *Brain Struct Funct* **213**, 525-533.

[63] Lustig C, Snyder AZ, Bhakta M, O'Brien KC, McAvoy M, Raichle ME, Morris JC, Buckner R L (2003) Functional deactivations: change with age and dementia of the Alzheimer type. *Proc Natl Acad Sci U S A* **100**, 14504-14509.

[64] Petrella JR, Prince SE, Wang L, Hellegers C, Doraiswamy PM (2007) Prognostic value of posteromedial cortex deactivation in mild cognitive impairment. *PLoS One* **2**, e1104.

[65] Sorg C, Riedl V, Muhlau M, Calhoun VD, Eichele T, Laer L, Drzezga A, Forstl H, Kurz A, Zimmer C, Wohlschlager AM (2007) Selective changes of resting-state networks in individuals at risk for Alzheimer's disease. *Proc Natl Acad Sci U S A* **104**, 18760-18765.

[66] Bai F, Zhang Z, Yu H, Shi Y, Yuan Y, Zhu W, Zhang X, Qian Y (2008) Default-mode network activity distinguishes amnestic type mild cognitive impairment from healthy aging: a combined structural and resting-state functional MRI study. *Neurosci Lett* **438**, 111-115.

[67] Buckner RL, Snyder AZ, Shannon BJ, LaRossa G, Sachs R, Fotenos AF, Sheline YI, Klunk WE, Mathis CA, Morris JC, Mintun MA (2005) Molecular, structural, and functional characterization of Alzheimer's disease: evidence for a relationship between default activity, amyloid, and memory. *J Neurosci* **25**, 7709-7717.

[68] Pengas G, Hodges JR, Watson P, Nestor PJ (2010) Focal posterior cingulate atrophy in incipient Alzheimer's disease. *Neurobiol Aging* **31**, 25-33.

[69] Chetelat G, Desgranges B, de la Sayette V, Viader F, Eustache F, Baron JC (2003) Mild cognitive impairment: Can FDG-PET predict who is to rapidly convert to Alzheimer's disease? *Neurology* **60**, 1374-1377.

[70] Anchisi D, Borroni B, Franceschi M, Kerrouche N, Kalbe E, Beuthien-Beumann B, Cappa S, Lenz O, Ludecke S, Marcone A, Mielke R, Ortelli P, Padovani A, Pelati O, Pupi A, Scarpini E, Weisenbach S, Herholz K, Salmon E, Holthoff V, Sorbi S, Fazio F, Perani D (2005) Heterogeneity of brain glucose metabolism in mild cognitive impairment and clinical progression to Alzheimer disease. *Arch Neurol* **62**, 1728-1733.

[71] van den Heuvel M, Mandl R, Luigjes J, Hulshoff Pol H (2008) Microstructural organization of the cingulum tract and the level of default mode functional connectivity. *J Neurosci* **28**, 10844-10851.

[72] Greicius MD, Supekar K, Menon V, Dougherty RF (2009) Resting-state functional connectivity reflects structural connectivity in the default mode network. *Cereb Cortex* **19**, 72-78.

[73] van den Heuvel MP, Mandl RC, Kahn RS, Hulshoff Pol HE (2009) Functionally linked resting-state networks reflect the underlying structural connectivity architecture of the human brain. *Hum Brain Mapp* **30**, 3127-3141.

[74] Bosch B, Arenaza-Urquijo EM, Rami L, Sala-Llonch R, Junque C, Sole-Padulles C, Peña-Gómez C, Bargallo N, Molinuevo J L,Bartres-Faz D (2010) Multiple DTI index analysis in normal aging, amnestic MCI and AD. Relationship with neuropsychological performance. *Neurobiol Aging*, in press.

[75] Fellgiebel A, Muller MJ, Wille P, Dellani PR, Scheurich A, Schmidt LG, Stoeter P (2005) Color-coded diffusion-tensor-imaging of posterior cingulate fiber tracts in mild cognitive impairment. *Neurobiol Aging* **26**, 1193-1198.

[76] Zhang Y, Schuff N, Jahng GH, Bayne W, Mori S, Schad L, Mueller S, Du AT, Kramer JH, Yaffe K, Chui H, Jagust WJ, Miller BL, Weiner MW (2007) Diffusion tensor imaging of cingulum fibers in mild cognitive impairment and Alzheimer disease. *Neurology* **68**, 13-19.

[77] Bai F, Zhang Z, Watson DR, Yu H, Shi Y, Yuan Y, Qian Y, Jia J (2009) Abnormal integrity of association fiber tracts in amnestic mild cognitive impairment. *J Neurol Sci* **278**, 102-106.

[78] Chua TC, Wen W, Chen X, Kochan N, Slavin MJ, Trollor JN, Brodaty H, Sachdev PS (2009) Diffusion tensor imaging of the posterior cingulate is a useful biomarker of mild cognitive impairment. *Am J Geriatr Psychiatry* **17**, 602-613.

[79] Kiuchi K, Morikawa M, Taoka T, Nagashima T, Yamauchi T, Makinodan M, Norimoto K, Hashimoto K, Kosaka J, Inoue Y, Inoue M, Kichikawa K, Kishimoto T (2009) Abnormalities of the uncinate fasciculus and posterior cingulate fasciculus in mild cognitive impairment and early Alzheimer's disease: a diffusion tensor tractography study. *Brain Res* **1287**, 184-191.